Propagation of Wide-Band Signals at VHF/UHF

ALAN G. CAMERON, SENIOR MEMBER, IEEE

Abstract—**The experimental jam-resistant secure voice communications (JRSVC) system developed by M.I.T. Lincoln Laboratory was used to conduct a series of VHF/UHF (225–400 MHz) propagation measurements, representative of a veriety of tactical communications situations, both ground to ground and ground to low-flying aircraft. Results are unusual in two regards: they were made with the receiver in motion, covering many contiguous propagation paths, and the JRSVC system, by frequency-hopping over almost an octave and averaging the results, largely eliminated the effects of frequency-selective (multipath) fading that generally dominate VHF/UHF propagation measurements.**

I. Introduction

THE ECCM ADVANTAGES of very wide-band radio transmission are well understood [1]–[3] and frequently exploited in modern military communications systems [4], [5]. Another advantage, not so fully appreciated, is the relative insensitivity to multipath-induced (frequency selective) signal fading of such wide-band transmissions. This was shown clearly in a recent series of VHF/UHF (225–400-MHz) propagation measurements made with the experimental Jam-Resistant Secure Voice Communications (JRSVC) system, designed and built by M.I.T. Lincoln Laboratory. Both ground-to-air and ground-to-ground propagation measurements were made in geometries representative of a variety of tactical situations. Due to the wide-band nature of the JRSVC signals (almost an octave), effects of multipath propagation, which often dominate propagation measurements at these frequencies, were greatly reduced, and signal levels were determined principally by physical obstructions along the propagation path. As a result, measurements were highly repeatable and agreed very closely with calculated predictions.

II. The JRSVC System

Three JRSVC half-duplex VHF/UHF transceivers (Fig. 1) were conceived, developed, built, and tested by M.I.T. Lincoln Laboratory in 1978–1982, in response to U.S. Air Force needs. The units were experimental, intended to investigate a variety of anti-jamming techniques, and were internally instrumented to record on magnetic tape a variety of parameters, including received signal strength on every frequency within the bandwidth to which the JRSVC signal hops.

Much of the detail of JRSVC operation is classified, and is well-covered in the classified literature. It suffices here to note that the JRSVC radio is a half-duplex push-to-talk voice transceiver, functionally very similar to today's conventional AM radio set, but possessing a high degree of jamming resistance and full security. It employs a time-hopping frequency-hopping pseudonoise hybrid waveform comprised of a rapid sequence of short pseudonoise bursts, each with 6 MHz instantaneous bandwidth (Fig. 2), transmitted on a center frequency chosen from among 32, spaced at 4 MHz intervals across the military UHF communications band. The particular 32 center frequencies used in these tests were 260, 264, 268, $\cdots$, 320, 324, 340, 344, 348, $\cdots$, 388, 392, and 396 MHz; the space between 324 and 340 MHz occupied by the glideslope portion of the civil ILS system was avoided. The JRSVC transmitter employs a fractional duty cycle with 40 W peak power. An additional high-power amplifier with 300 W (peak) output was used in some tests.

Individual transmission bursts are time-shared between the functions of synchronization and information transmission. Synchronization bursts occur in groups of three throughout the transmission, which the receiver combines and performs detection upon, to enable initial acquisition and tracking of received signals. There is no synchronization preamble. Information-bearing bursts each carry 8 bits of voice information. Voice encoding and decoding employs standard 16 kbit/s continuously variable slope delta (CVSD) modulation, whose performance is sufficiently good at high error rates to preclude the need for any error detection or correction coding, even against partial-band interference. It should be apparent that such insensitivity to disruption of small fractions of the transmission is a prerequisite to the full realization of the multipath fading resistance of wide-band operation.

The frequency of the JRSVC receiver (Fig. 3) is determined by a programmable fast-hopping frequency synthesizer hopped in synchronism with the received signal. The receiver employs dual conversion with 200- and 32-MHz intermediate frequencies, and synchronous conver-

Manuscript received October 9, 1984; revised February 8, 1985. This work was sponsored by the Department of the Air Force. The views and conclusions contained in this document are those of the contractor and should not be interpreted as necessarily representing the official policies, either expressed or implied, of the United States Government.

The author was with M.I.T. Lincoln Laboratory, Lexington, MA 02173. He is now with Teledyne Brown Engineering, Lexington, MA 02173.

0733-8716/85/0756$01.00

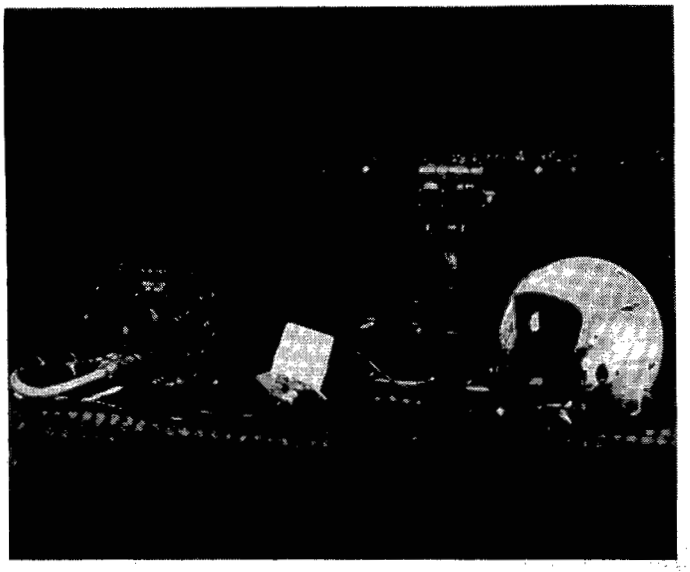

Fig. 1. The JRSVC transceiver.

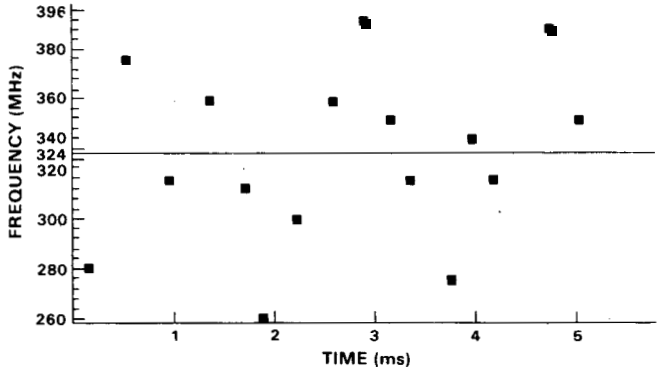

Fig. 2. JRSVC waveform.

sion from the second intermediate frequency to baseband in-phase and quadrature channels. These baseband signals are fed to charge-coupled device (CCD) matched filters which extract the voice and timing information from the pseudonoise signal. Receiver operation is linear with fast AGC (time constant of a few microseconds) up to the (linear) matched filter. All AGC action occurs at 32 MHz; receiver dynamic range extends from -20 to -100 dBm (the noise threshold) prior to that point. Matched filter outputs are digitized and fed to a fast general-purpose microcomputer for further processing. Other functions performed as well by the microcomputer include control of receiver and matched filter hardware, code and pseudonoise sequence control and handling, synchronization processing, received signal detection and deciphering management, and performance data extraction and formatting.

To allow direct measurement of received signal level for performance testing, the receiver is tapped at the 32 MHz intermediate frequency at a level approximately 10 dB above that of the antenna input; the tapped output is fed to a separate power-level measuring instrumentation receiver, comprised of a log video amplifier, low-pass filter (approximately 20 μs settling time), and analog-to-digital converter. Converter sampling time is controlled by the microcomputer to ensure that it is performed in synchronism with the received signal, and that peak signal power level is sampled at a stable point within each burst. The sampling process operates on every burst and sampled power level values are written continually into a set of 32 locations in the JRSVC microcomputer memory, corresponding to the 32 frequencies over which the signal hops. Previously stored values are overwritten. Once every 256 ms, the data extraction software reads the (most recently measured[1]) contents of the 32 locations, along with a variety of other parameters, for output to magnetic tape. Recorded instrumentation data includes: power-level measurements made while the received signal is present on each of the 32 frequencies (as noted above); other background (nonsignal) power across the band determined by the same measurement process, but made when JRSVC signals are absent; received signal timing (to 1/8 μs); the presence of additional signals (due, for example, to long time delay multipath); channel voice data error rate (using a special "test pattern" which can be transmitted in lieu of voice); system status (control settings, etc.); synchronization detection statistics; and a variety of other parameters useful in determining system performance. Magnetic tapes containing these data are processed and reduced to a variety of formats after the experiment is performed, by an ECLIPSE-based operator-interactive data analysis facility at Lincoln Laboratory. Formats include numerical printouts, spectrum plots, and plots of level versus time, either on a set of selected frequencies or averaged over the entire frequency band.

The analog-to-digital converter in the JRSVC instrumentation receiver provides 8-bit output, linear in dBm (due to the logarithmic amplifier), with about three counts per decibel. The 8-bit words are processed through calibration tables, each tailored to an individual receiver, in the data reduction software. Average power across the frequency band is calculated by converting measured data in dBm to watts, averaging those and reconverting the result back to dBm. Estimated overall accuracy of the pathloss measurement process is better than ± 2 dB.

To summarize those JRSVC parameters pertinent to the experiments, the system transmits and receives a wide-band (6 MHz) signal over 32 frequencies, spaced 4 MHz apart within the UHF band, from 260 to 396 MHz (with a 12 MHz gap from 324 to 336 MHz). The receiver measures the power received on each frequency, averaged over 20 μs, and provides data which, when suitably processed, yields the average value of the power received on all frequencies. That value is converted to dBm in the data presented here.

III. The Experiments

Two series of experiments pertaining to propagation were conducted: a flight test program in the Rome, NY

[1]The frequency-hopping pattern used for these tests ensured that all level data were measured within 15 ms of the time of output.

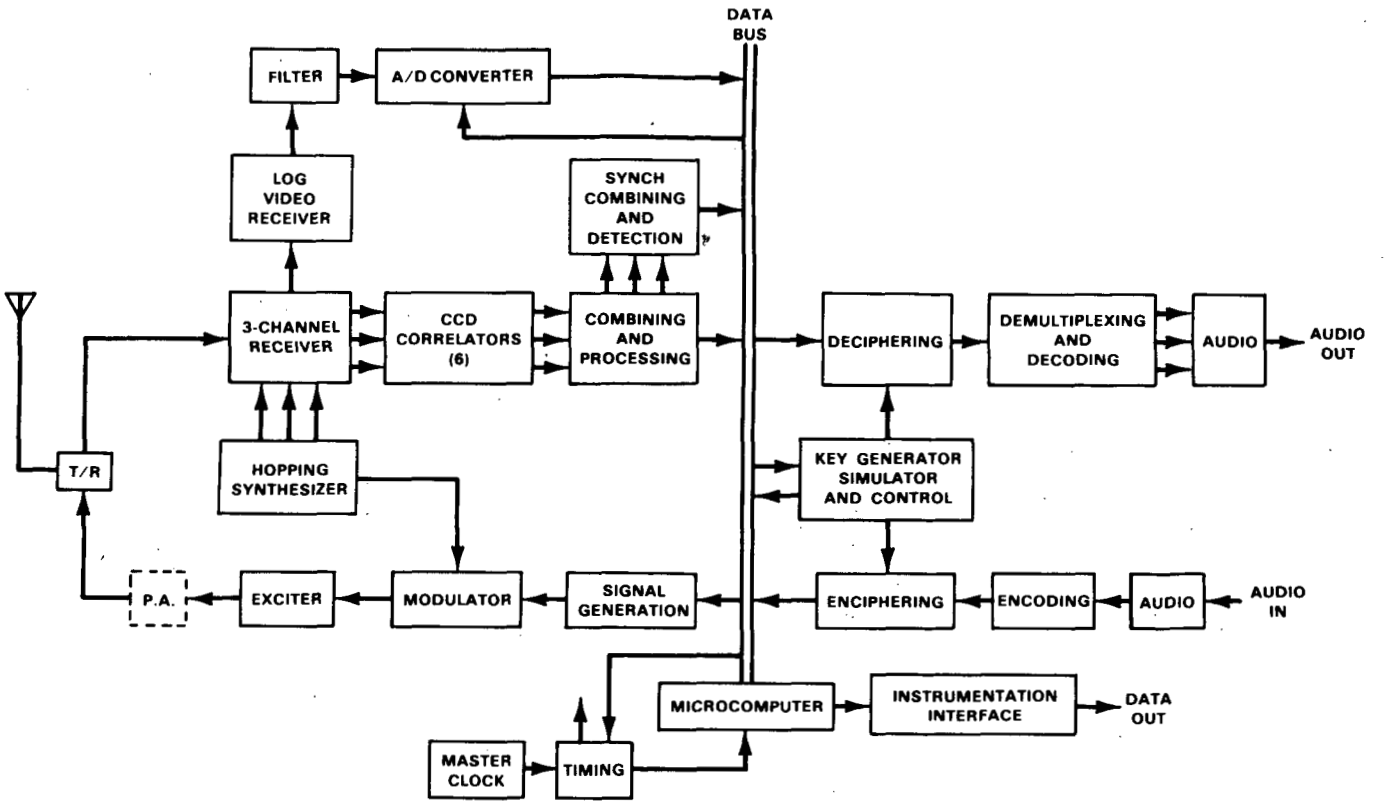

Fig. 3. JRSVC transceiver block diagram.

area in the Fall of 1982, and a series of ground-to-ground tests involving a mobile van, conducted during 1982–1983 in the Lexington, MA area.

A. Ground-to-Ground Testing

Evaluation of the operational suitability of systems such as JRSVC involves, among other things, the use of propagation models for ground-to-ground transmission paths, along which pathlosses can be considerably greater than freespace calculations would indicate. Models used for preliminary JRSVC evaluation, which presumed a smooth finitely-conducting spherical earth, suggested link failure at ranges on the order of 8–12 nmi, with 300 W peak power, far below what had been noted in field testing. Accordingly, a series of ground-to-ground propagation tests were performed to better characterize wide-band signal propagation effects, and to support the development of more accurate models.

The measurements reported here were made between a JRSVC transmitter located at M.I.T. Lincoln Laboratory in Lexington, MA with a rooftop pole-mounted broad-band "discone" omnidirectional antenna, and a mobile receiver mounted in a van (Fig. 4) with a similar antenna. The equipment in the van was powered by an auxiliary generator, capable of operation while the van was in motion. The experimental program was performed over a 10-month period during 1982–1983, and so encountered a full variety of propagation-related environmental conditions (e.g., foliage, snow).

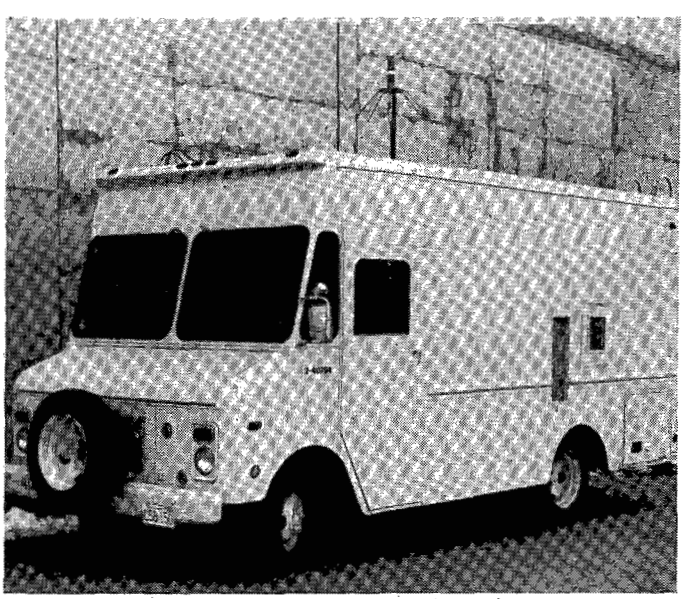

Fig. 4. Mobile transceiver installation.

An ideal experiment would involve driving the van along a radial path, as in flight testing. Lacking such a path to the desired distance in a direction with significant topography, we observed that Massachusetts State Route 2 extends more or less radially from the transmitter site (Fig. 5), varying in azimuth from the transmitter site by less than 20° out to 40 nmi. Within that region, elevation varies as shown in Fig. 6. It should be emphasized that because the

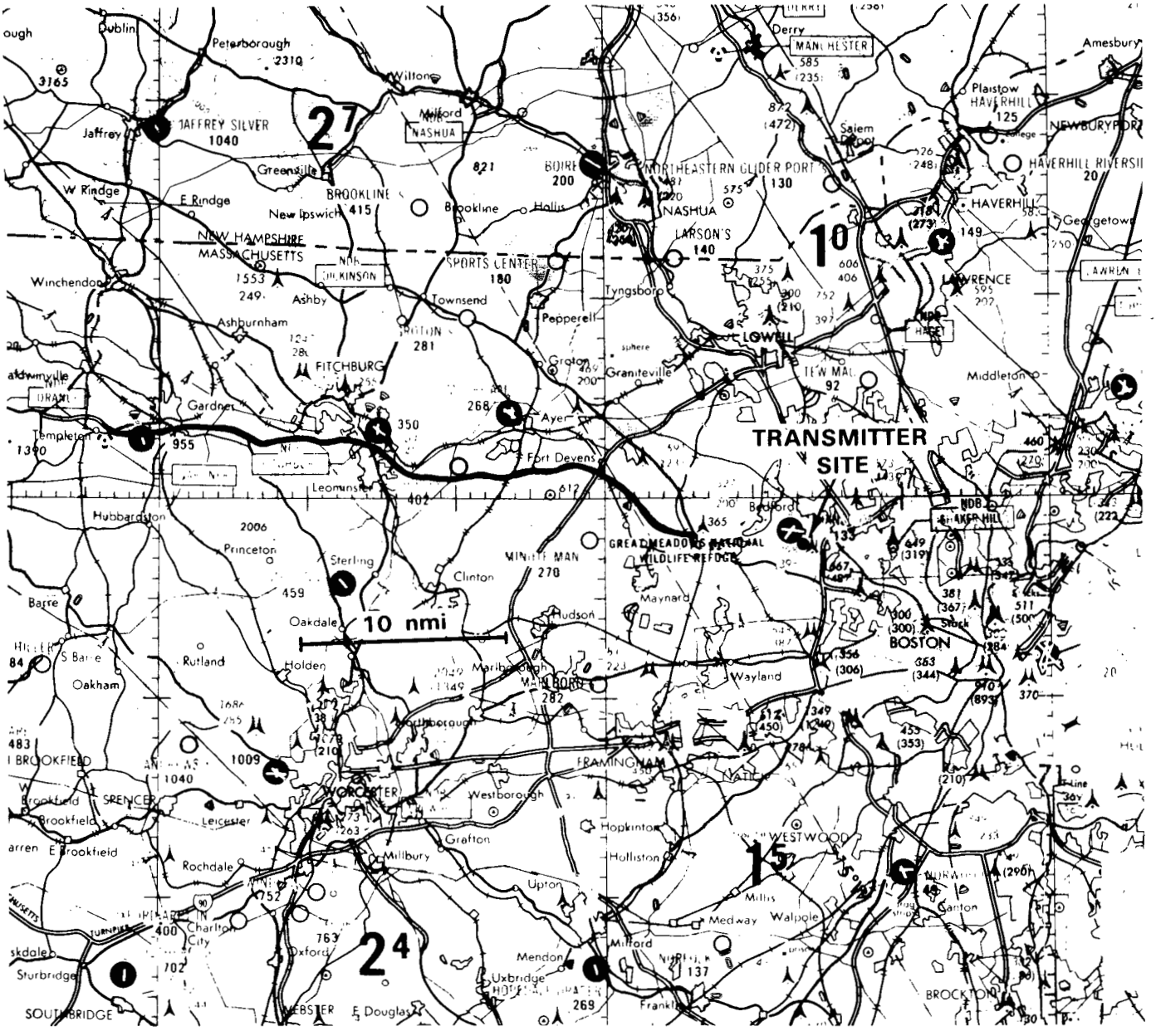

Fig. 5. Path along which measurements were made.

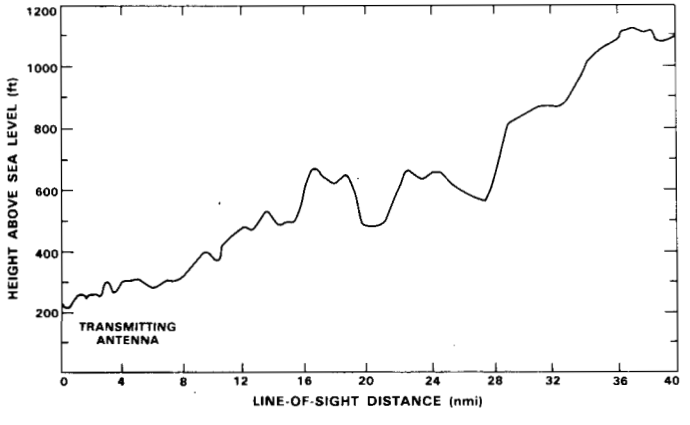

Fig. 6. Elevation along path of Fig. 5.

route is not purely radial, this is not an accurate propagation path profile. In general, the transmitting site, as viewed by the receiver, did not lie directly back along the road, but varied by as much as $\pm 45°$ from the van's instantaneous "heading." Thus, the propagation profile from many points along the route included trees, buildings, and terrain in the immediate vicinity of the highway, whose characteristics were not easily determinable. Fortunately, there were exceptions to this situation.

Fig. 7 is a complete plot of measured (frequency-averaged) signal level along the route to the point where permanent loss of signal occurred; these data were collected in wintertime, with no snow on the ground and no leaves on the trees. Note that the data exhibit two types of characteristic behavior: rapid fluctuation in most places

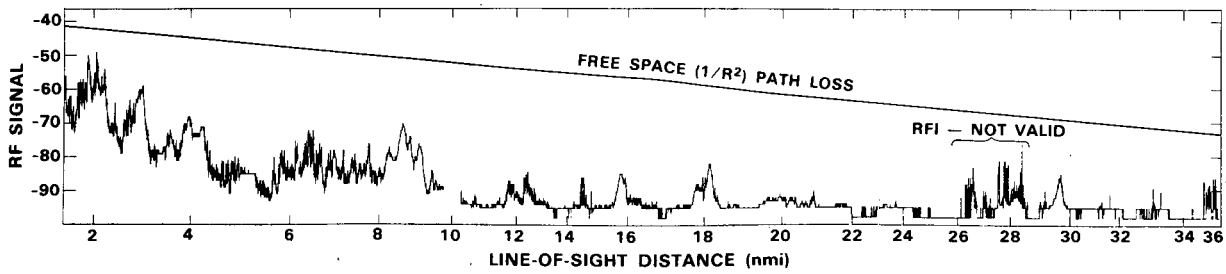

Fig. 7. Signal level measured along path of Fig. 5.

and relatively slow variation elsewhere. At longer ranges, signal level falls below that of receiver noise, and accurate propagation losses can no longer be determined. The lowest level on the plot indicates loss of signal; this occurred in low spots at relatively close range, and became more prevalent at longer range. Permanent dropout occurred at about 40 nmi.

Correlation of the data with the immediate surroundings of the van along the route revealed that the relatively smooth portions of the data occurred when the view of the horizon from the van in the direction of the transmitter was relatively low, not changing rapidly, with minimal obstruction in the foreground. Since this generally occurred on hillsides, it was generally associated with an increase in signal level.

The more rapid fluctuations in the data appear due primarily to blockage caused by obstructions along the roadside, whose characteristics vary rapidly as the van moves past them, rather than due to multipath propagation. Multipath propagation is indeed present but the wide-band nature of the measurement process again appears to be effectively reducing it. This can be seen in Fig. 8, which is an expanded plot of a portion of the data of Fig. 7, between 1 and 2 nmi from the transmitter, where the direction to the transmitter varies between $\pm 45°$ from the perpendicular to the direction of the van.

Fig. 8(a)–(c) presents levels measured on individual frequencies: 280, 320, and 376 MHz; Fig. 8(d) is the average power level across the band calculated and plotted as in Fig. 7. Note the preponderance of large rapid multipath-induced fades (over 10 dB between adjacent points) in the individual frequency data, which appear independent among the different frequencies, and how the more well-behaved average data of Fig. 8(d) appear to underlie all of them.

Individual frequency fading is not deeper because the individual frequency signals are still fairly broadband. Recall that the JRSVC waveform is a hybrid of time hopping, frequency hopping, and pseudonoise. The pseudonoise process results in a bandwidth of approximately 6 MHz, which limits fade depth to about 20 dB even in the ideal case where a CW signal at the center frequency would be completely cancelled.

That the fluctuations remaining after frequency averaging are due to physical obstructions along the path can also be seen by examination of data taken in repeated experiments along the same path. Fig. 9(a)–(e) presents data

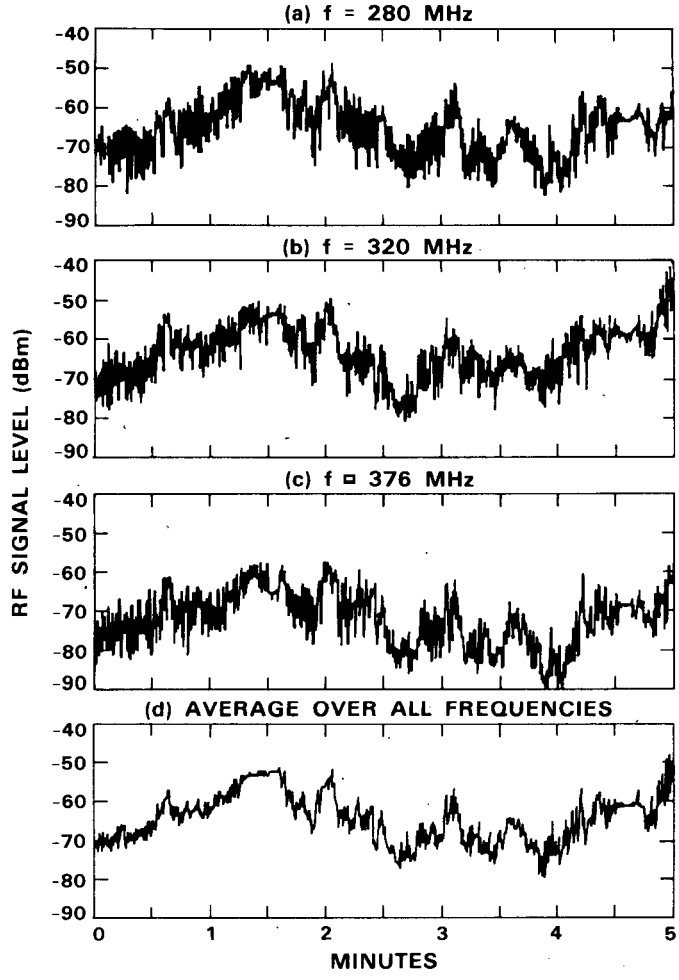

Fig. 8. Levels measured on several individual frequencies. (a) $f = 280$ MHz. (b) $f = 320$ MHz. (c) $f = 376$ MHz. (d) Average over all frequencies.

taken along the Route 2 path under various conditions, as enumerated in Table I. It is evident that these data are highly repeatable, even in the fine structure. The few differences in the shape of the various plots are primarily the horizontal "plateaus" of varying lengths, sometimes altogether absent. Data, although presented as a function of distance along the route are, of course, recorded as a function of time and the gross assumption is made that distance increases monotonically with time as the scale indicates (different scales on the different data resulting from different van speeds). The "plateaus" are due to unplanned stops at traffic lights.

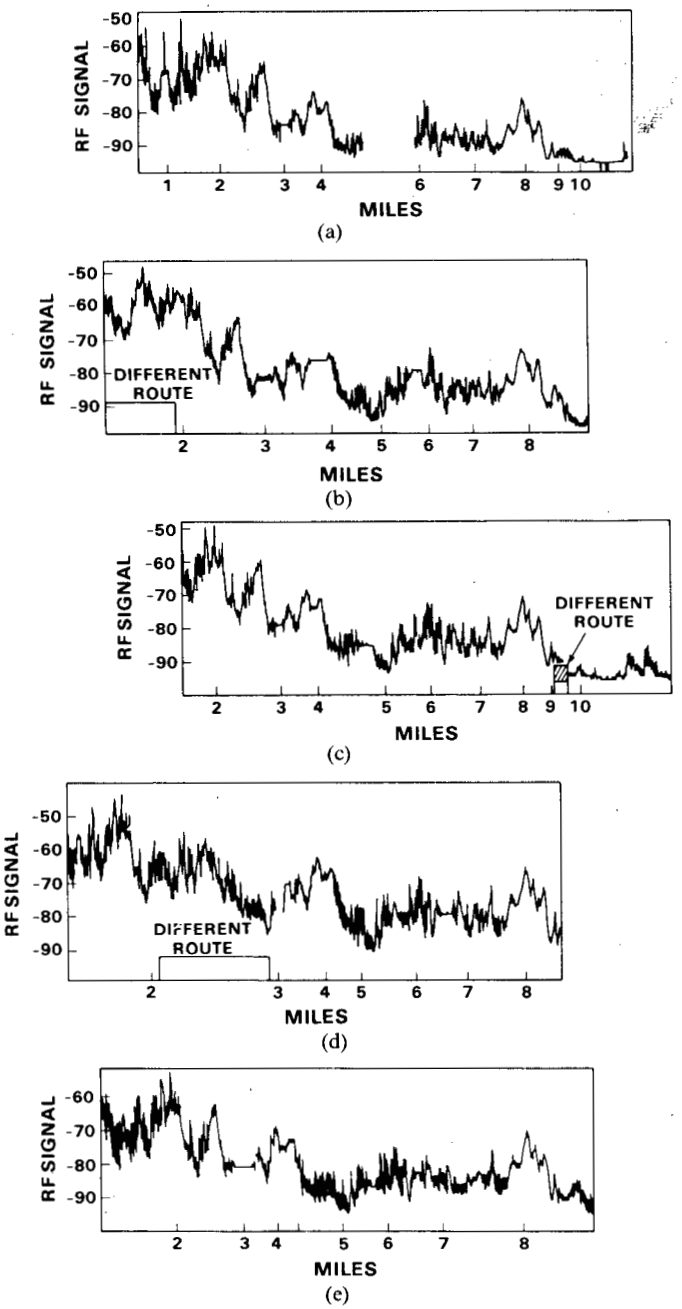

Fig. 9. Data from several runs along path of Fig. 5. (a) Test 50. (b) Test 52. (c) Test 53. (d) Test 60. (e) Test 61.

Note that the data presented in Fig. 9 were taken with leaves on/off the trees, and snow on/off the ground. Some of the variations in the patterns are presumably due to these differences. To establish effects on overall propagation, several easily distinguishable points on the individual plots were selected (for example, two peaks at 1 nmi, the leftmost peak at 5 nmi, the deepest null at slightly under 1 nmi), and levels at these points compared. No significant differences were observed; levels at each point were in all cases within 1 dB of one another among all five sets of data.

Two segments of the data, both free from foreground obstructions, were selected for further analysis. These were

TABLE I
DATA COLLECTION RUNS ALONG ROUTE 2

Test Number	Date	Power	Conditions
50	12/28/82	Low	Cold, dry, no snow, no leaves
52	1/2/83	High	Cold, sunny, no snow, no leaves
53	2/23/83	High	Raining, snow, no leaves
60	10/3/83	High	Clear, warm—leaves on
61	10/14/83	High	Clear, cool—leaves falling

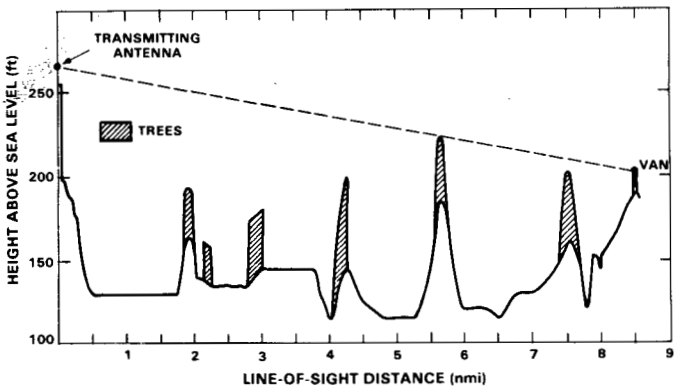

Fig. 10. Profile of path to the $8\frac{1}{2}$ mi point.

the peak at $8\frac{1}{2}$ nmi, which occurred on a low hill relatively free from obstruction, where the transmitter lay directly behind the van, and the peak at 15 nmi, which occurred about halfway up a long hill, where the horizon in the direction of the transmitter was again quite low. (Above that point, the highway curved behind nearby terrain.)

A multitude of pathloss prediction models exist, embodying a variety of assumptions about what underlying propagation effects are dominant, and requiring varying degrees of knowledge of the parameters of the particular propagation path of interest. Meeks [6] recently conducted an extensive study of those models appropriate to the civil VHF radionavigation band (108–118 MHz), and concluded that despite the relative flatness of the topography in Eastern Massachusetts, diffraction over hills was nonetheless a dominant effect, and thus a multiple knife-edge diffraction model [7], due to Deygout, was more appropriate to the terrain than models assuming a smooth Earth [8]. He confirmed this experimentally [9], [10] in terrain near where these tests were conducted. Thus the Deygout model was applied to the two sets of data.

Fig. 10 is the terrain profile along the path to the $8\frac{1}{2}$-nmi site; Earth curvature, which introduces at worst an 8 ft error, has been neglected. This path is in some instances more than a mile north of the traveled route; thus the profile is quite different from Fig. 6. The profile includes an obstruction, a hill $5\frac{1}{2}$ mi from the transmitter, which just grazes the line-of-sight path, and two additional hills within one fresnel zone of the path. (Hill elevations were taken from topographic maps; tree heights were estimated by eye. Meeks established that trees are definitely a factor at these frequencies and must be included.)

The Deygout model requires the construction of the diffraction path involving the highest obstacle (here the

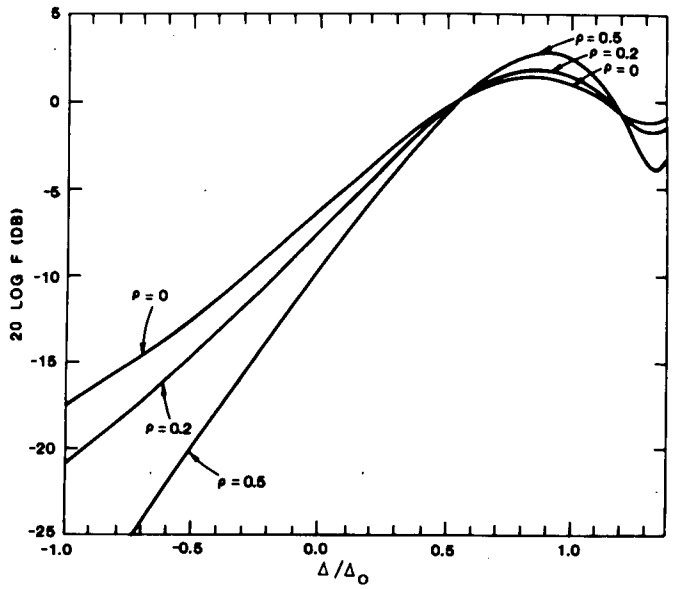

Fig. 11. Functional relationship between normalized clearance (Δ/Δ_0) and additional loss (F) (for several radii of curvature, ρ).

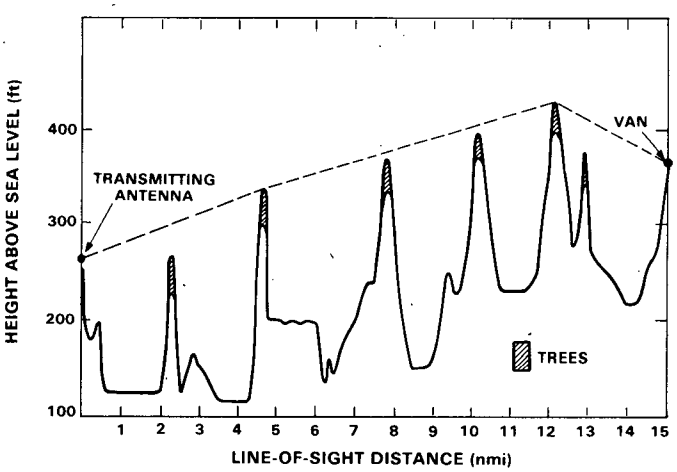

Fig. 12. Profile of path to the 15 mi point.

line-of-sight path itself, since the highest obstacle just grazes it), and the calculation of correction factors for all significant obstacles as a function of their distances from the diffraction path (both above and below). This relationship is plotted in Fig. 11 (from Meeks [6]), where F is the excess pathloss due to the obstruction, and Δ/Δ_0 is the clearance between the line-of-sight path and the obstacle (negative if the obstacle actually impinges across the path), normalized relative to the clearance of the first fresnel zone. The model allows for several assumptions about the "sharpness" of the hills; the "knife-edge" and "cylinder with characteristic radius-of-curvature $\rho = 0.2$" assumptions appeared most appropriate to this topography.[2]

[2] The characteristic radius of curvature, ρ, is given by [11]

$$\rho = \frac{1}{\Delta_0}\sqrt[3]{\frac{\lambda^2 r}{\sqrt{\pi}}}$$

where r is the actual radius of curvature of the hill.

Signal level is estimated by summing the correction factors (in decibels) pertinent to the obstacles and adding them to freespace ($1/R^2$) pathloss. The "knife-edge" model predicts a 14-dB excess loss over freespace pathloss; assuming $\rho = 0.2$ results in 17.5 dB excess loss. Measured signal levels were found to be between 17 and 19 dB below freespace, for this 8 mi path.

Fig. 12 is a profile of the path to the 15 mi point. This path is roughly 8° north of the previous path, and encounters an entirely different set of terrain obstructions. Most are hills with relatively round cross section, and the propagation path grazes along the sides of the two most significant ones. That is, when viewed from the transmitter their "knife-edges" are not horizontal. This introduces a bit of uncertainty into their heights and suggests a three-dimensional propagation geometry, somewhat more complex than what Deygout considered.

Nonetheless, the Deygout model yields relatively good results. Taking into account the five highest obstacles and making the same assumptions about foliage height as before, the model yields excess losses of 31.5 and 37.5 dB for the "knife-edge" and $\rho = 0.2$ cases, respectively. Measured excess pathloss was 27 dB.

There are several error sources in the measurement process, which could explain the small spread of the results: measurement inaccuracy should contribute less than 2 dB, as should receiving and transmitting antenna patterns. Near-field transmitting antenna obstructions (primarily other antennas, masts, towers, and other obstacles on the laboratory roof) could account for small variations in signal level that differ in the two directions. In addition, topographic estimates are somewhat uncertain, especially with regard to tree heights. The hills involved in both paths were examined only visually; they are all tree-covered and tree heights were estimated to be uniformly 40 ft, typical of the second-generation forest that predominates in this area. Examination of Fig. 11 reveals that a 10 ft error in this estimate will produce a 1 dB error in these model results.

To determine the effects of different, less hilly topography, two data collection runs were preformed along Route 128 northbound (Fig. 13), which extends roughtly east-northeasterly from Lincoln Laboratory, through terrain that becomes gradually less hilly as it approaches the coast. Whereas typical hills were 150–200 ft above the surrounding valleys along the Route 2 path, the figure was more typically 50–100 ft along Route 128 north. Fig. 14 is a plot of elevation along the route, and Fig. 15(a) and (b) presents the data collected along the two runs. The sharp spikes at 9 and 12 nmi are due to interference from other sources (they were present in data taken at instants when the signal was absent), and should be ignored.

Again, the signal level exhibits broad, relatively smooth peaks on hilltops and more rapid variation in the proximity of obstructions. The series of notches in the 1–2 nmi region occurred as the van passed beneath a series of underpasses along Route 128, the wide notch at 2.6 nmi corresponding to a wide (four-lane highway) underpass. Deygout analysis was performed on data from the hill at 8 nmi, and resulted in excess pathloss 2 dB less than what was measured.

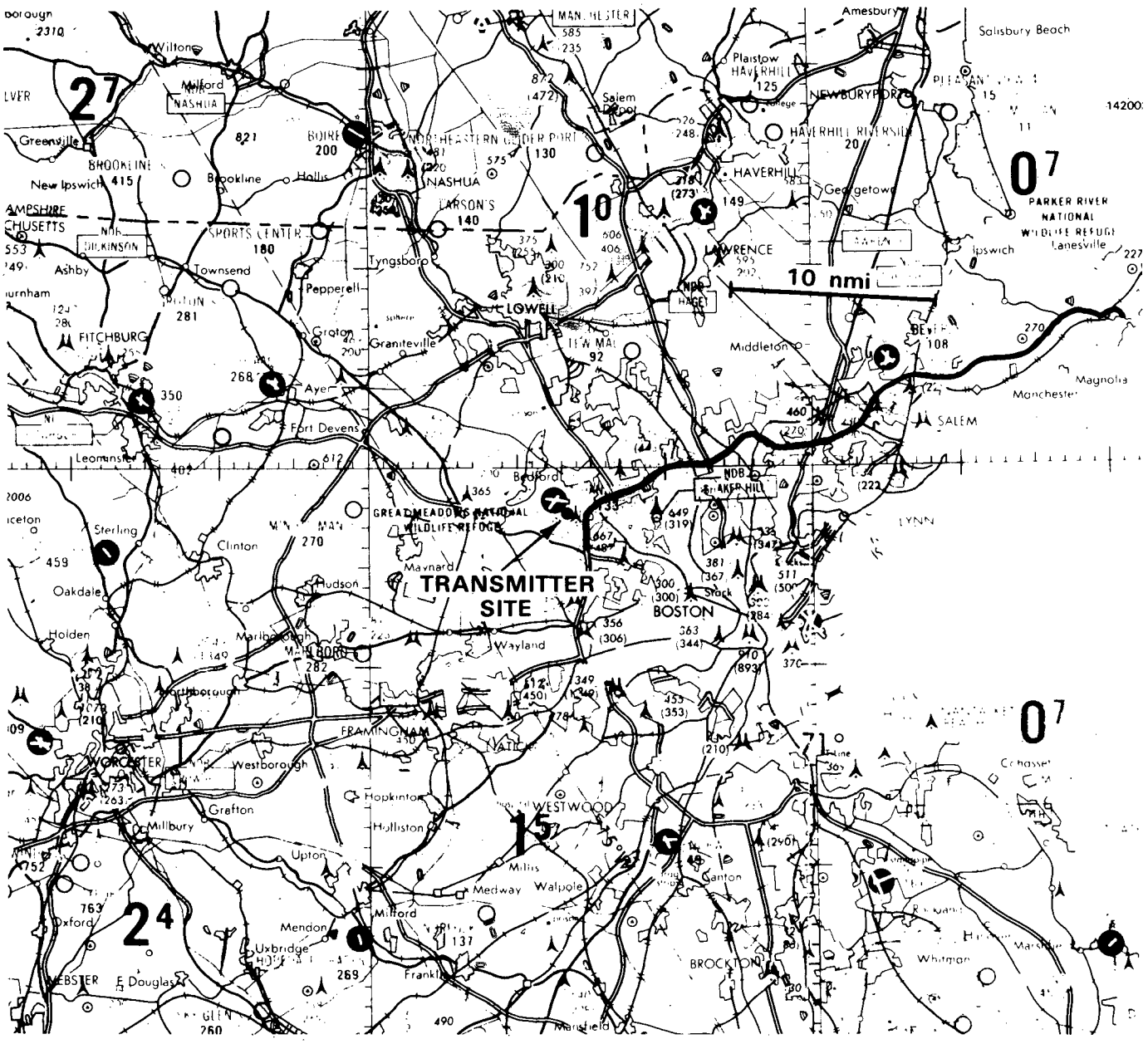

Fig. 13. Path along Route 128 North.

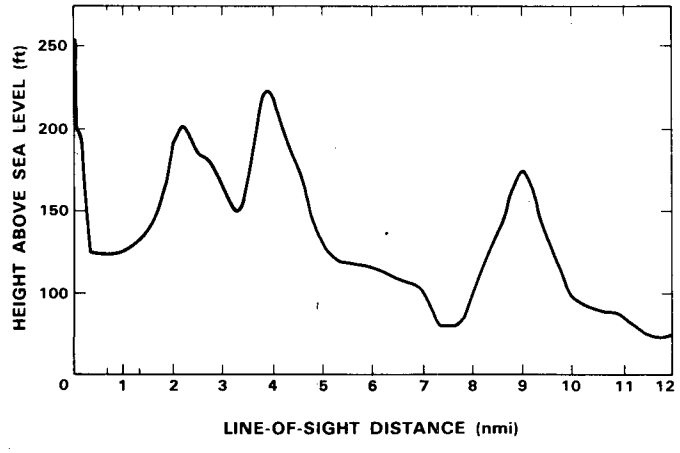

Fig. 14. Elevation along Route 128 North.

B. Ground-to-Air Propagation

Flight testing was concerned primarily with the determination of JRSVC system performance against jamming, and involved flight paths that brought the airborne JRSVC receiver into close proximity of a jammer installation. Prior to conducting those tests, however, several flights were made without any jamming to investigate signal propagation and establish signal levels along the flight path.

The JRSVC transmitter was located in a building at the Rome Air Development Center Verona (NY) test site with a pole-mounted rooftop omnidirectional broad-band antenna. The antenna foreground in the direction of the flight path was clear (mowed grass) flat and unobstructed for about $\frac{1}{2}$nmi, where it was broken by a treeline. The antenna was 36 ft above the level of this ground.

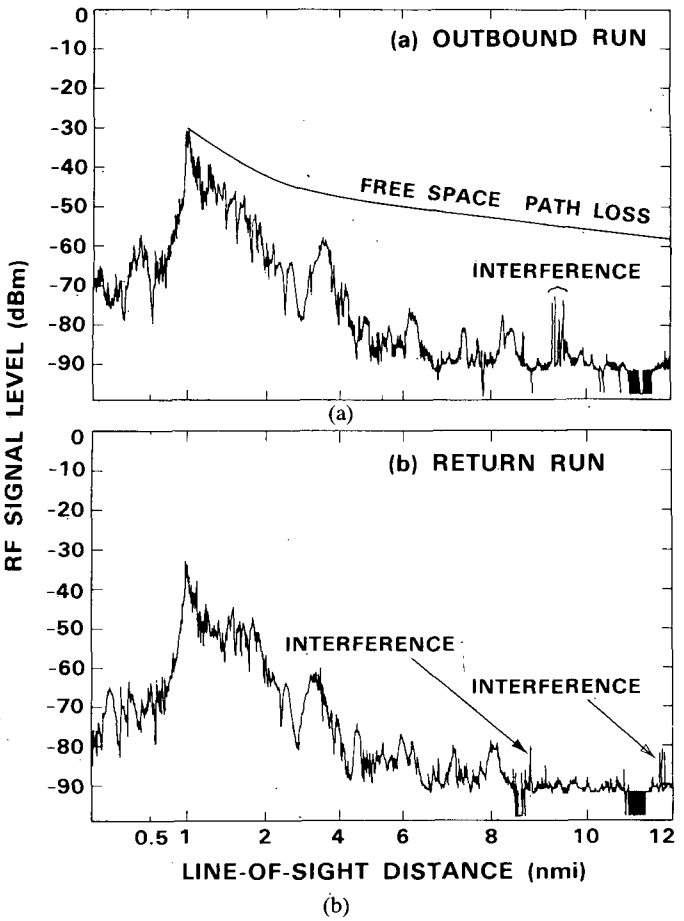

Fig. 15. Levels measured along Route 128 North. (a) Outbound run. (b) Return run.

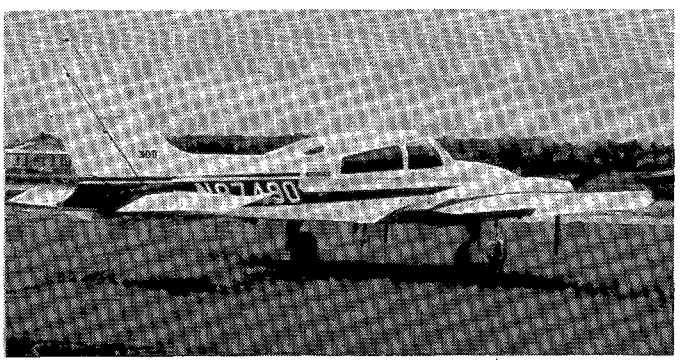

Fig. 16. Airborne JRSVC transceiver installation.

The airborne receiver was installed in a Cessna 310 light twin-engine aircraft (Fig. 16) with a belly-mounted omnidirectional UHF blade antenna.

Fig. 17 shows the test flight geometry. Because the foreground of the ground transmitting antenna is flat out to 3000 ft, noticeable multipath interference effects (so-called "vertical lobing") would be expected, with the first-order null (pathlength difference of one wavelength at the center of the signal bandwidth, 330 MHz) intersecting the flight path 8.14 nmi from the transmitter site.

A narrow-band CW signal at 330 MHz would exhibit a fairly deep null at this location, due to partial cancellation of the direct and reflected signals. Null depth would depend on the reflection coefficient of the ground; it was not easily measurable, but a value around -0.8 (corresponding to a 14 dB null), commonly attributed to a situation such as this [6], is certainly consistent with the observed data. Fig. 18 shows received (frequency-averaged) JRSVC signal levels measured along the flight path on seven different passes. Note that no sharp nulls are present in this data, and that the data are highly correlated from one pass to the next, varying at any particular location by at most a few decibels. Note also the relative freedom from rapid fluctuation; levels change slowly and steadily, rarely by more than 1 or 2 dB from one sample point to the next. Also note that with the exception of the region between 6 and 10 nmi from the source, levels are within ± 3 dB of what free-space pathloss calculations would predict, with no allowances whatsoever for fading.

The reduction in signal level below the calculated level by 3–6 dB in the region between 6 and 10 nmi is due to vertical lobing; if the foreground were perfectly flat and level, and the phase change upon reflection were exactly 180°, the first order-null would occur at the lower edge of the JRSVC signal bandwidth, 260 MHz, at 6.4 nmi and at the upper edge, 400 MHz, at 9.8 nmi. Between those two points, the null would move gradually across the signal bandwidth. Since the bandwidth is slightly less than one octave (and since the transmitted signal level and antenna aperture are not perfectly uniform across the band), the loss of signal due to partial cancellation in this region is not totally compensated by the additional power in the lobes of the ground antenna pattern (due to partial reinforcement of the direct signal by the multipath signal), and some net loss occurs. This can be seen in the signal

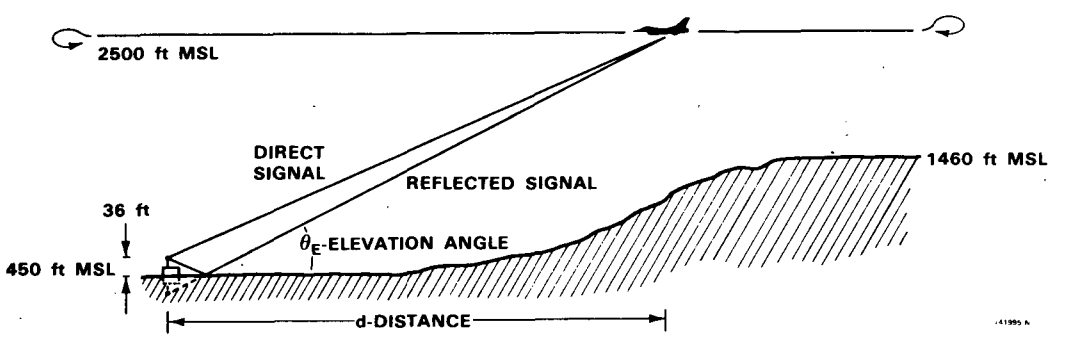

Fig. 17. Test flight geometry.

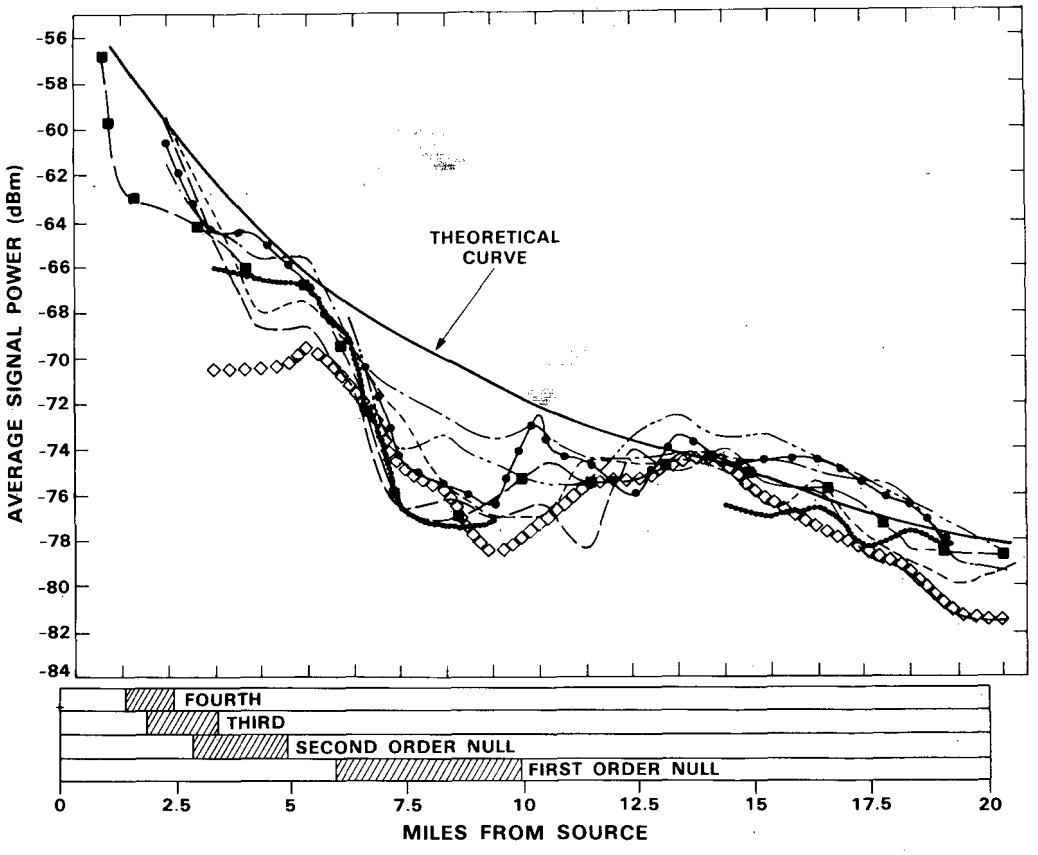

Fig. 18. Levels measured along flight path.

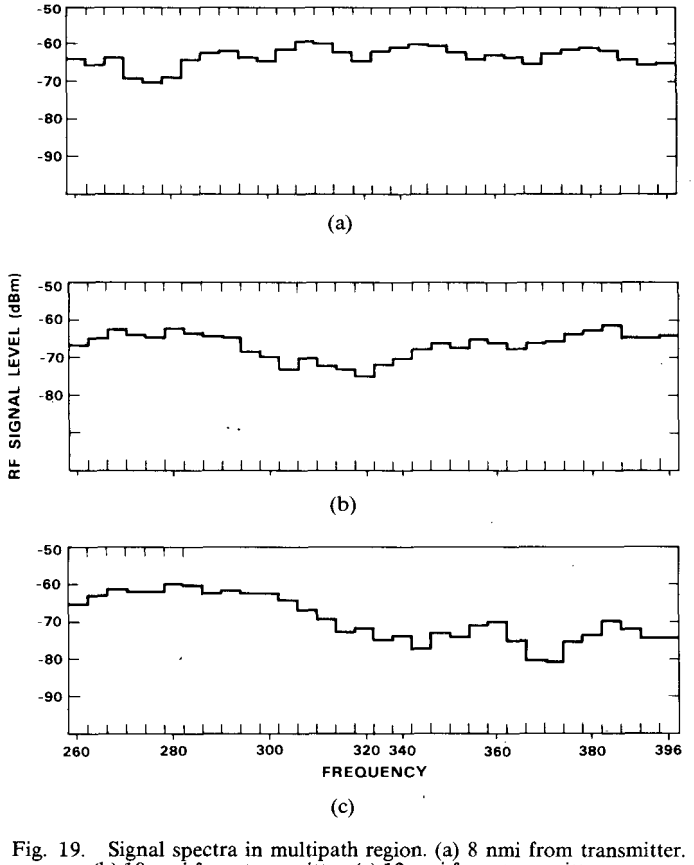

Fig. 19. Signal spectra in multipath region. (a) 8 nmi from transmitter. (b) 10 nmi from transmitter. (c) 12 nmi from transmitter.

spectrum plots of Fig. 19, taken at various ranges within the region where the first-order null is present.

IV. Conclusions

The wide bandwidth (in terms of percentage of the center frequency) over which the JRSVC system operates makes possible the collection of received signal-level data which is almost completely free from the deleterious effects of short time delay multipath-induced frequency-selective fading. It also provides the opportunity, if design steps are taken to minimize susceptibility to the loss of small portions of the received signal, to eliminate these effects from system operational performance.

When the effects of multipath fading have been removed, the underlying data is well behaved and repeatable, and correlates well with physical obstructions along the propagation path. Even in relatively flat regions like Eastern Massachusetts, diffraction over what small hills are present is the dominant propagation mechanism, and signal level is given accurately by the Deygout method. Since eastern Massachusetts is hardly representative of the rest of the world, it is difficult to generalize these results to many other locations. On the other hand, since the Deygout method yields such accurate results in this relatively flat region, it would appear the appropriate choice for estimating propagation losses in other, hillier terrain.

Topographic characteristics in this area are consistent with a rough prediction rule-of-thumb: excess pathloss grows linearly in dB at a rate of about 2 dB per nautical mile, to 30 dB at 15 nautical miles, and remains constant beyond that. Similar rules-of-thumb for other regions could likely be developed by determining topographical characteristics from charts, and applying Deygout's method to them.

ACKNOWLEDGMENT

Many people involved in the development and testing of the JRSVC system contributed to the experimental program reported here. J. U. Beusch and R. W. Bush actively encouraged and supported it, C. E. Holborow participated in it, and designed and developed much of the data reduction software. M. L. Meeks furnished expertise and interest. A. Matlin performed the data reduction, and assembled the data presented, and S. M. Tobin and D. Daly participated in the data collection and maintained the JRSVC equipment in perfect condition at all times. L. M. Wesley provided editorial assistance in the preparation of this paper.

REFERENCES

[1] R. C. Dixon, *Spread-Spectrum Systems*, New York: Wiley, 1976.
[2] R. A. Scholtz, "The origins of spread-spectrum communications," *IEEE Trans. Commun.*, vol. COM-30, p. 822, May 1982.
[3] "Progress in spread-spectrum communications," *Rec. 1982 Military Commun. Conf.* (MILCOM), sponsored by the IEEE, DoD, AFCEA, Oct. 1982.
[4] N. B. Hemesath and W. M. Hutcheson, "*GPS overview and user equipment antijam design*," *Int. Telemetry Conf. Proc.*, vol. XIV, 1978.
[5] W. F. Lynch, "TDMA JTIDS overview description," MITRE, Tech. Rep. 8413 (AD-B066 309L), June 1982.
[6] M. L. Meeks, *Radar Propagation at Low Altitudes*. Dedham, MA: Artech House, 1982.
[7] J. Deygout, "Multiple knife-edge diffraction of microwaves," *IEEE Trans. Antennas Propag.*, vol. AP-14, pp. 480–489, 1966.
[8] M. A. Maiuzzo and W. E. Frazier, "A theoretical ground-wave propagation model—Nλ model," ESD-TR-68-315 (AD-845 720L), Dec. 1968.
[9] M. L. Meeks, "VHF propagation over hilly, forested terrain," Proj. Rep. CMT-19 (AD-A115 746), Lincoln Laboratory, M.I.T., Lexington, MA, Apr. 9, 1982.
[10] M. L. Meeks, "VHF propagation near the ground: An initial study," Proj. Rep. CMT-35 (AD-A122 498), Lincoln Laboratory, M.I.T., Lexington, MA, Oct. 26, 1982.
[11] H. T. Dougherty and L. J. Maloney, "Application of diffraction by convex surfaces," *Radio Sci.*, vol. 68D, pp. 239–250, 1964.

Alan G. Cameron (S'59–SM'84) was born in Pawtucket, RI, in 1940. He received the B.S. and M.S. degrees from the Massachusetts Institute of Technology, Cambridge, in 1962 and 1964, respectively.

He served in the U.S. Navy from 1964 to 1966 as an engineering duty officer. Upon release from active duty he joined the technical staff of the MITRE Corporation, where he worked on a variety of communications and avionics programs. He has been a staff member at M.I.T. Lincoln Laboratory since 1972, with activities in radar, radar beaconry, and spread-spectrum communications. His interests include systems analysis, ECM/ECCM analysis and design, and system performance testing.

Mr. Cameron is a member of Eta Kappa No, Sigma Xi and Tau Beta Pi.